

# Impedance Matching and Implementation of Planar Space-Filling Dipoles as Intraocular Implanted Antennas in a Retinal Prosthesis

Keyoor Gosalia, *Member, IEEE*, Mark S. Humayun, *Member, IEEE*, and Gianluca Lazzi, *Senior Member, IEEE*

**Abstract**—In this work, an extremely compact planar meander line dipole is designed and implemented for use as an intraocular element in a retinal prosthesis. This planar meander dipole antenna exhibits a high degree of current vector alignment and is impedance matched by inducing a current phase reversal along its length. This current phase reversal is induced by a minor offset in feed location which yields a highly directive broadside radiation pattern on this particular planar antenna geometry. This concept is applied in designing and implementing a  $6 \times 6$  mm planar compact wire dipole at 1.4 GHz as the intraocular element for the data telemetry link of a retinal prosthesis. Coupling measurements between an external microstrip patch antenna and the intraocular wire dipole are presented and compared with those obtained with intraocular microstrip patch antennas in place of the wire dipole. It is demonstrated that such compact meander dipoles can perform better than previously reported microstrip patch antennas as intraocular elements for a retinal prosthesis.

**Index Terms**—Implanted antennas, miniature antennas, planar meander dipole antennas, retinal prosthesis.

## I. INTRODUCTION

A retinal prosthesis is a rehabilitative implantable device being designed to restore a limited form of vision in the blind suffering from retinal degenerative diseases. This dual unit device employs an external unit to capture visual information which is transmitted to the unit implanted in the eyeball – or intraocular unit – using a wireless telemetry link. After requisite signal processing in the implanted microchip, an electrode array stimulates the surviving retinal cells to achieve visual perception. The physiological basis and functionality of such a prosthetic device has been well reported [1]–[5] and will not be described in detail here. In our previous work, the feasibility of establishing a wireless microwave data telemetry link for such a visual prosthesis using external and implanted microstrip patch antennas was demonstrated [6].

One of the proposed solutions for the intraocular device is the implanted antenna and electronics (RF receiver, data processing and signal stimulator chips) reside on the same Si substrate.

Manuscript received December 16, 2004; revised April 26, 2005. This work was supported in part by NSF CAREER award ECS-0091599, in part by the Whitaker Foundation under Grant RG-00-0298, and in part by the NSF under Grants EEC-0310723 and ECS-0335537.

K. Gosalia is with General Dynamics C4 Systems (Satcom Technologies), Kilgore, TX 75662 USA.

M. S. Humayun is with the Doheny Retina Institute, Keck School of Medicine, University of Southern California, Los Angeles, CA 90033 USA.

G. Lazzi is with the Department of Electrical Engineering, North Carolina State University, Raleigh, NC 27695 USA (e-mail: lazzi@ncsu.edu).

Digital Object Identifier 10.1109/TAP.2005.852514

Such a configuration of the intraocular elements could be packaged in a single unit and it would require limited space inside the eyeball. In this particular configuration, the secondary coil required for the power transfer link will surround the intraocular unit. In such a scenario, a microstrip antenna solution as intraocular data telemetry antenna as reported in [6] would have two drawbacks. Specifically, since the secondary coil would enclose the ground plane of the microstrip antenna, the mutual flux linkages with the external coil and hence the coupling efficiency for power transfer may be adversely affected. Further, since a metal ground plane is needed for the microstrip antenna, it would be necessary to bond a metal layer (aluminum, Al) to the silicon wafer, adding complexity to the fabrication process.

Therefore, it is necessary to consider alternative compact antenna configurations as intraocular radiating elements to account for effects of system integration. A class of antennas which are devoid of ground planes and can perform as effective compact radiators are wire dipoles. In this paper, we present compact wire dipoles as intraocular radiating elements and the techniques to miniaturize them for the visual prosthesis application. The following points are carefully addressed: a) determine if compact wire dipole can, in fact, provide the high degree of compactness essential for the proposed application; b) determine if these compact wire structures could be impedance matched to the desired system resistance at their resonance frequency (since an important characteristic of compact wire geometries is the reduction in resonant resistance with increasing compactness); c) compare the suitability of these planar meander line wire dipoles with that of fractal geometries.

We observed that though the fractal geometries can provide the requisite compactness but impedance matching increases the complexity in the feed location for such an antenna configuration and the proposed application. Therefore, we utilize a planar meander line dipole antenna and propose a technique to impedance match the antenna at any real impedance without additional complexity while retaining the feed point location at its symmetric center. Its implementation for a visual prosthesis is discussed and it is shown that, at a frequency of approximately 1.4 GHz, the wire antenna element (with dimensions within  $6 \times 6 \times 1.5$  mm) as the intraocular receiving structure may, in fact, improve the performance of the data telemetry link as compared with the intraocular microstrip patch antenna. Several results and plots are presented which compare the coupling results obtained with the receiving (intraocular) wire and patch antennas. It should be noted that this work

deals with the design and implementation of a receiving wire antenna for the wireless telemetry link, and the patch antenna results have been adapted from [6] only to facilitate a performance comparison between the two types of intraocular receiving antennas.

This paper is organized in the following sections. Section II outlines the antenna design and computational results for a prototype structure. Implementation for a retinal prosthesis is discussed in Section III. The inductive influence of the eye model and the corrective measures taken are described in Section IV. Section V compares the coupling results obtained with this intraocular wire dipole antenna with those of the intraocular microstrip patch antenna. The conclusions are presented in Section VI.

## II. ANTENNA DESIGN AND COMPUTATIONAL RESULTS

Recently, it has been demonstrated that the resonant behavior of any space-filling wire antenna is a function of all of its physical characteristics which include its geometry, overall size, total wire length and wire diameter [7]. Also, the effectiveness of any antenna in lowering resonant frequency is dependent on current vector alignment in parallel, closely coupled, sections of wires in its geometry [8]. For the intraocular radiating element of a retinal prosthesis, we investigated a space-filling geometry of a meander line dipole with a high degree of current vector alignment as shown in Fig. 1(a).

To gain an insight on the physical behavior of such an antenna, the prototype antenna for the computational study measured  $52.5 \times 52.5$  mm (the side length is scaled down by 10 times in the actual intraocular antenna as described later) and is designated as A0. Its wire diameter was  $10 \mu\text{m}$  with a total wire length of  $0.75875$  m. The wire was considered to be perfectly conducting devoid of any losses for this work. Its numerical investigation was performed using the NEC 2 engine of NEC Win-PRO [13] where it was modeled using 607 segments each having a length of 1.25 mm. It exhibited its impedance characteristics as shown in Fig. 1(b).

Here, the current vectors along parallel adjacent coupled sections of wire reinforce to increase the self-inductance and hence lower the resonant frequency lending this structure a very high compression efficiency as compared to the Hilbert curve [8]. Moreover, it should be noted that the quality factor  $Q$ , or the antenna's radiative usefulness was not the focus of this study and hence is not discussed in detail. However, as is later observed, the prototype exhibits a  $kr < 0.2$  (much smaller than a radian length; where  $k$  is the wavenumber and  $r$  is the radius), and when operated at its higher order mode, this antenna shows very high directive gain at the expense of bandwidth leading to a very high  $Q$  radiator. This performance is consistent with what has been reported over the last few decades [9]–[12].

### A. Impedance Matching for Planar Meander Dipole

1) *Conventional Matching Technique:* At its fundamental resonance, the phase remains almost constant along the length of the wire and it can be matched in the conventional way by moving the feed point toward the wire end [14]. Antenna A0 was matched at its fundamental resonant frequency, by selecting an off-center feed point and moving it along the

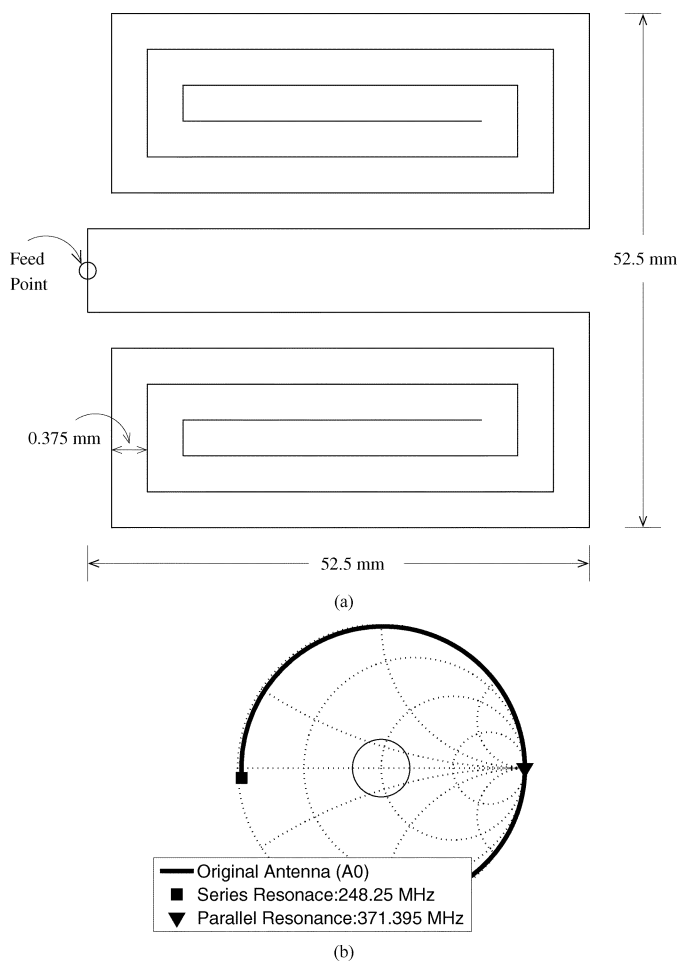


Fig. 1. Planar meander dipole antenna configuration: (a) The prototype A0 considered for NEC simulations (wire radius of  $10 \mu\text{m}$ ) and (b) impedance characteristics of A0 with the feed point at the symmetrical center.

length of the wire until a good match to  $50 \Omega$  was obtained. This planar dipole was designated as A1 and the match was achieved with the feed point positioned at segment 18 from the wire end of one of the arms.

Fig. 2 shows the current vector alignment and impedance characteristics for the prototype antenna A1 matched with its feed location as depicted. The fundamental resonance for the prototype occurred at 248 MHz and a VSWR 3:1 bandwidth of 0.06% was observed. As seen from the figure, the current phase remains constant throughout the length of the dipole.

However, the conventional method of impedance matching presents the same complexity (arbitrary feed location) as was observed for other compact antenna geometries like the fractal antennas. The next subsection outlines the method of antenna matching by inducing a current phase reversal along the length by a minor offset in the feed location.

2) *Current Phase Reversal for Impedance Matching:* To explain the current phase reversal we first consider a simple full wave dipole of the same total wire length of  $0.75875$  m. It is well understood [15] that when the full wave dipole is fed a quarter wavelength from one end, it exhibits a current distribution that is significantly different (in terms of phase) from the center-fed full-wave dipole. When fed at quarter wavelength offset, due to the induced phase reversal, the dipole exhibits a series resonance

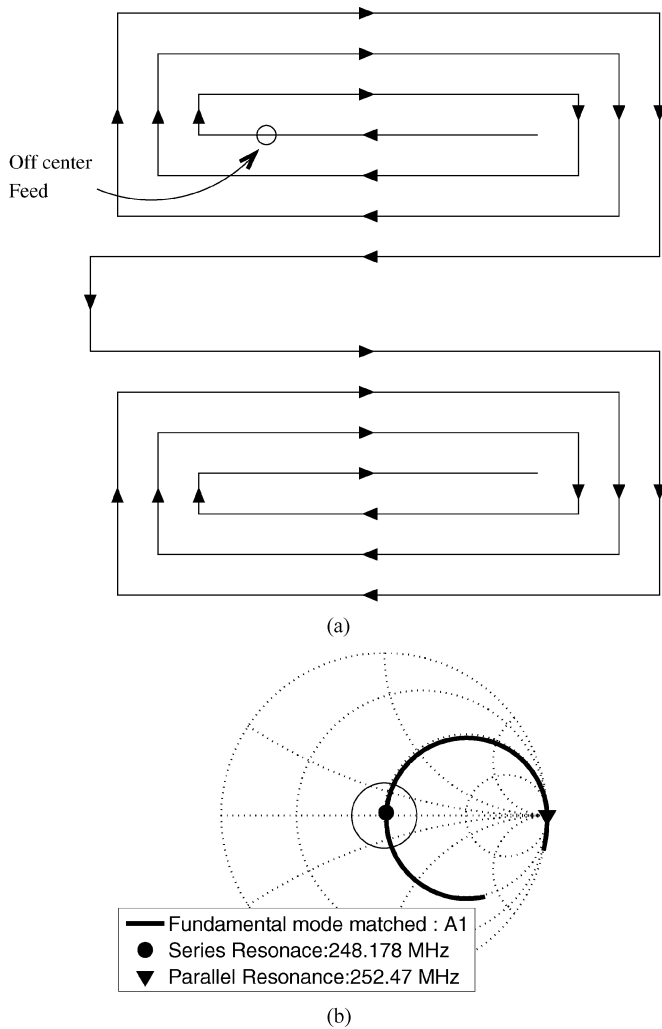


Fig. 2. Conventional impedance matching of the fundamental mode by moving the feed point toward the wire end-antenna A1: (a) Current vector alignment and feed point location and (b) impedance characteristics of A1.

at a frequency very close to the full-wave parallel resonance of the center fed dipole as shown in Fig. 3(a). The current phase reversal due to the off-center feed leads to broadside nulls which is an undesirable effect in the normal dipole. However, in the case of our planar meander line dipole, a phase reversal can improve the directivity in the broadside direction and provide an impedance match very close to the full-wave resonant frequency as is discussed below.

To impedance match the planar meander dipole antenna A0 by inducing a phase reversal, a minor offset had to be introduced in the location of the feed point. Instead of moving the feed point itself, one of the arms of the dipole was shortened to create the necessary minor offset in the feed point location. The dipole arm was shortened incrementally until the induced series resonance indicated a good match to 50 ohms. The impedance characteristics depicting the induced series resonance due to the off center feed is shown in Fig. 3(b).

In the prototype, the dipole arm was shortened by 2.5 mm (2 segment lengths) and the modified matched antenna was designated A2. Fig. 4(a) depicts the modified matched antenna A2 and the current phase reversal which occurs right at its center.

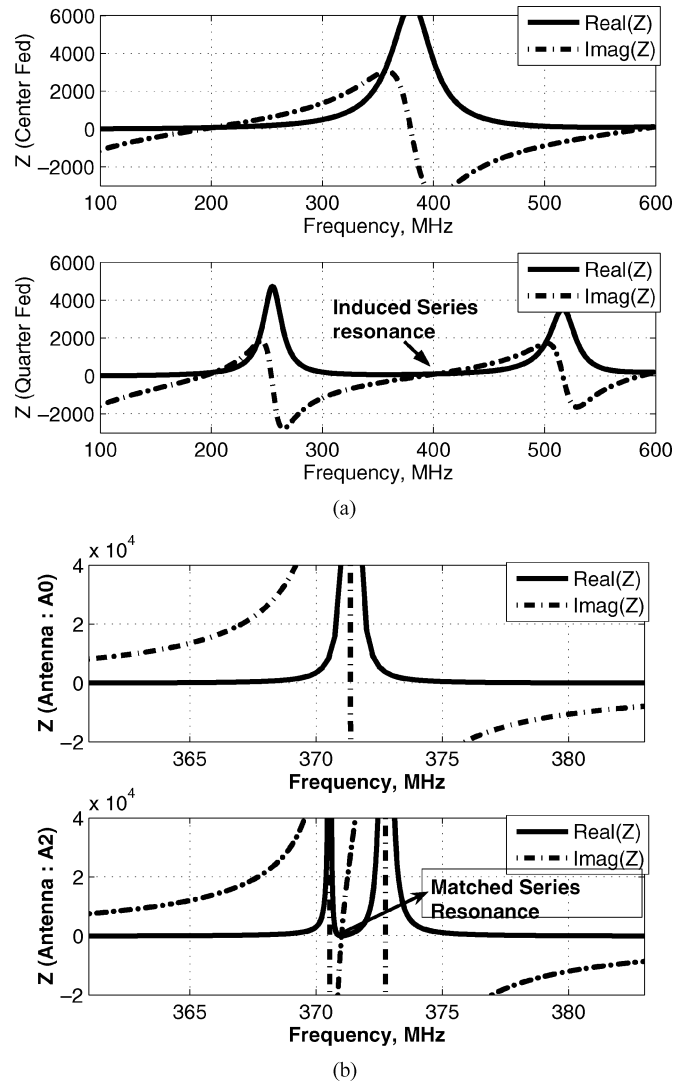


Fig. 3. Comparison of the impedance characteristics for center fed and off center fed dipole antennas; the off center feeding induces a series resonance for both the types of dipoles: (a) Center fed and quarter wave offset fed linear dipole and (b) center fed and a Minor offset fed meander line dipole.

Its impedance characteristics are shown in Fig. 4(b) where the meander dipole is matched at its induced series resonance.

The matched induced series resonance is obtained at 370.008 MHz for A2 which is very close to the unmatched full wave resonance of 371.395 MHz for the prototype antenna A0. (We observed that actually moving the feed point also leads to the same effect and that the exact amount of offset is very critical in obtaining a good match at the induced series resonance). The antenna could be matched at any resistance by controlling the amount of offset (or shortening of the arm) in the feed location. The bandwidth deteriorated significantly and for the prototype considered here, a VSWR 3:1 bandwidth of 0.0002% was observed.

Moreover, it was seen that the degree of offset (and hence the amount of shortening of the dipole arm) necessary for inducing a current phase reversal (immediately beyond its full wave resonant frequency) is dependent on the compression efficiency of the given antenna geometry. In [7] it was shown that due to the high level of current vector alignment in its parallel adjacent

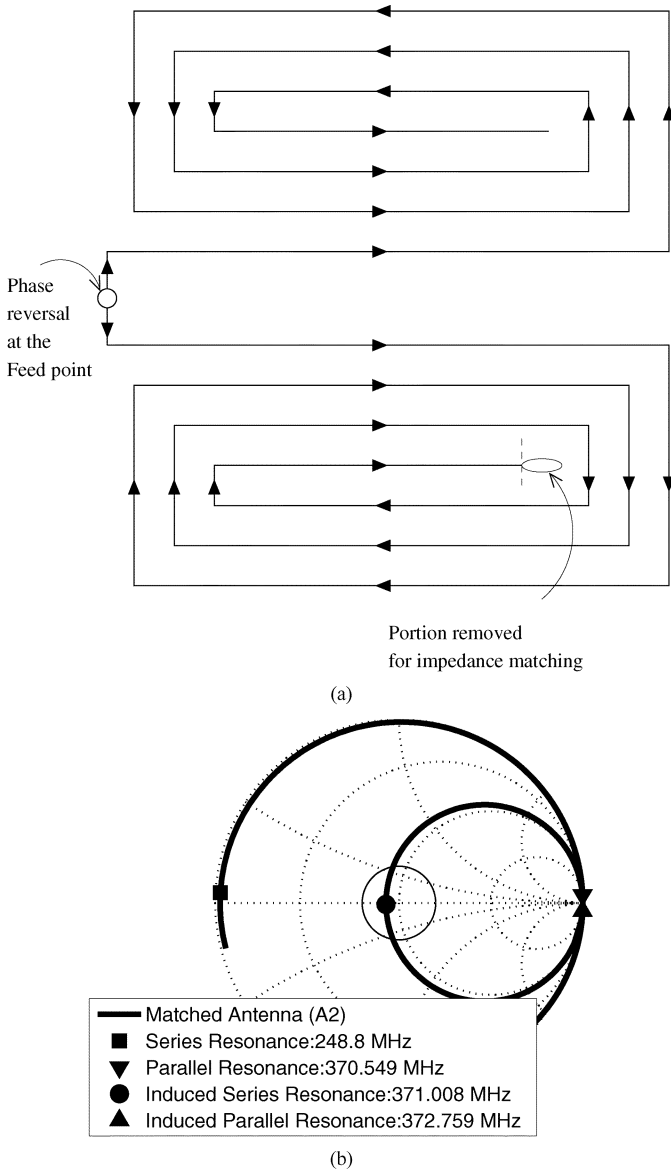


Fig. 4. Impedance matching the meander dipole by current phase reversal (while retaining the feed point at the edge)—Antenna A2: (a) Current phase reversal at the center due to minor feed offset and (b) impedance characteristics of A2 showing matching to  $50 \Omega$  at the induced series resonance.

arms, an antenna geometry such as A0 is much more efficient in lowering resonant frequency than a Hilbert curve fractal geometry. And, though it is not explicitly reported here, we observed that for a Hilbert curve (order 4) and a Sierpinski curve (order 5), which exhibit a lesser compression efficiency, a significant amount of dipole arm had to be shortened in order to induce a current phase reversal.

### B. Current Distribution and Radiation Pattern

Fig. 5 shows the current distribution (magnitude and phase) for antennas A1 and A2 at their respective matched frequencies. While there is a slight variation of phase along the length of A1 (at its fundamental mode), A2 depicts a phase reversal by 180 degrees approximately at its symmetric center.

Fig. 6(a) and (b) depict the radiation patterns due to antennas A0 (at its unmatched full-wave resonance) and A2 (at its matched series resonance). The radiation patterns are for both the antennas located in the  $xy$  plane. The phase reversal at the midpoint of A2 facilitates the specific current vector alignment as shown in Fig. 4(a) which contributes to a highly directive radiation pattern broadside to the plane of the antenna. It is observed from Fig. 6(a) and (b), that the radiation from A0 (with no phase reversal) is directed in the azimuthal plane while A2 focuses the radiation in the broadside direction.

Fig. 6(c) and (d) compares the radiation patterns of antennas A2 and A1 at their respective matched frequencies. Again, the maximum directivity of A1 conforms to the theoretically expected [15] value for small antennas of  $\sim 1.7$  dBi while for antenna A2 it is 5.16 dBi. It must be noted that the increase in directivity in Antenna A2 is compensated by a severe reduction in the impedance bandwidth.

We have observed that the method of current phase reversal to impedance match small antennas will improve broadside directivity only in specific cases (like antenna A2) on which the current vectors in adjacent wire segments are aligned favorably. Attempts at matching fractal antenna geometries of Hilbert (order 4) and Sierpinski curves (order 5) by current phase reversal did not yield any improvement in the directivity due to the arbitrary current vector alignment in fractals.

Fig. 7 depicts the total directivity patterns of the conventionally matched antenna A1 and antenna A2 matched by an induced current phase reversal at their respective frequencies.

### III. IMPLEMENTATION OF THE PLANAR MEANDER DIPOLE FOR A RETINAL PROSTHESIS

The prototypes studied in the NEC simulations measured  $52.5 \times 52.5$  mm and operated at approximately 370 MHz. For the retinal prosthesis, the implemented intraocular wire antennas had to operate at 1.4 GHz. This would enable a performance comparison between the patch and wire antennas as intraocular elements [6]. Moreover, the size had to be restricted to  $6 \times 6$  mm to enable implantation within the eyeball.

Therefore, the intraocular wire antennas were designed with dimensions of  $5.25 \times 5.25$  mm. In free space, the antennas operated at approximately 3.9 GHz (a 10 times increase in frequency of operation). Hence, a high dielectric constant of 9.2 was used with a thickness of 1.5 mm and the intraocular antennas were fabricated using standard PCB prototyping milling machines to operate at approximately 1.4 GHz. An unbalanced feed mechanism was used (SMA connectors) and the antennas were matched to  $50 \Omega$  by shortening one of the arms (as explained in the previous section). The final implemented matched intraocular wire dipoles operated at approximately 1.41 GHz and their resonance frequency was matched to that of the extraocular antenna (microstrip patch antenna) by adjusting the length of the arms.

A picture showing the implemented wire antenna and corresponding extraocular antenna (microstrip patch) operating at approximately 1.41 GHz is shown in Fig. 8. The experimental set up used for measurements was identical to the one described in [6].

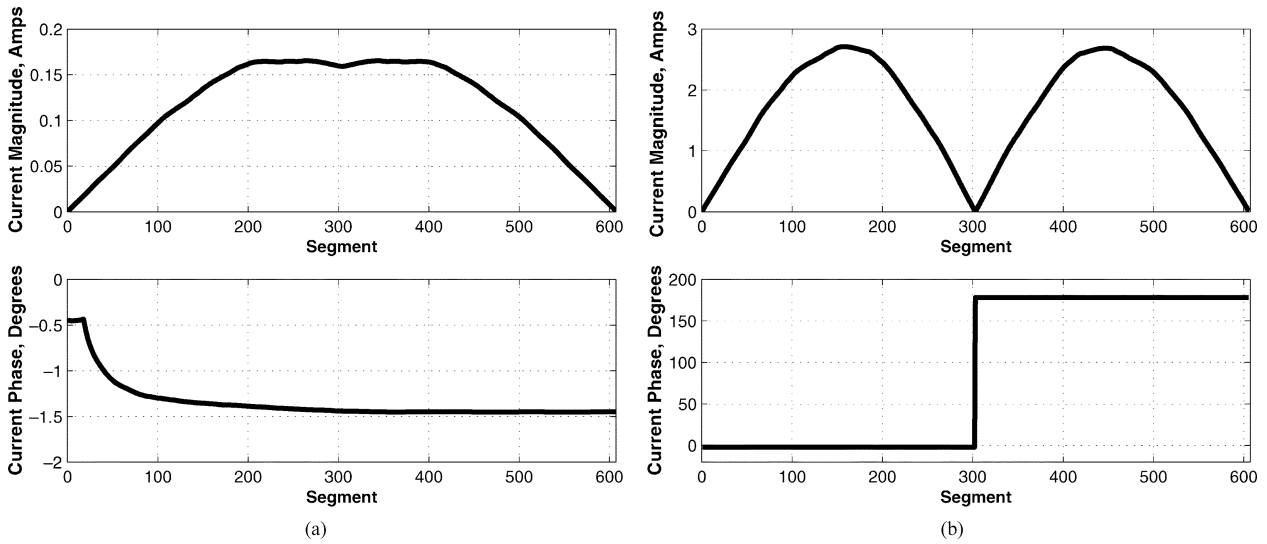


Fig. 5. Simulated current magnitude and phase distribution: (a) Antenna A1 (fundamental mode matched) and (b) antenna A2 (full wave mode matched).

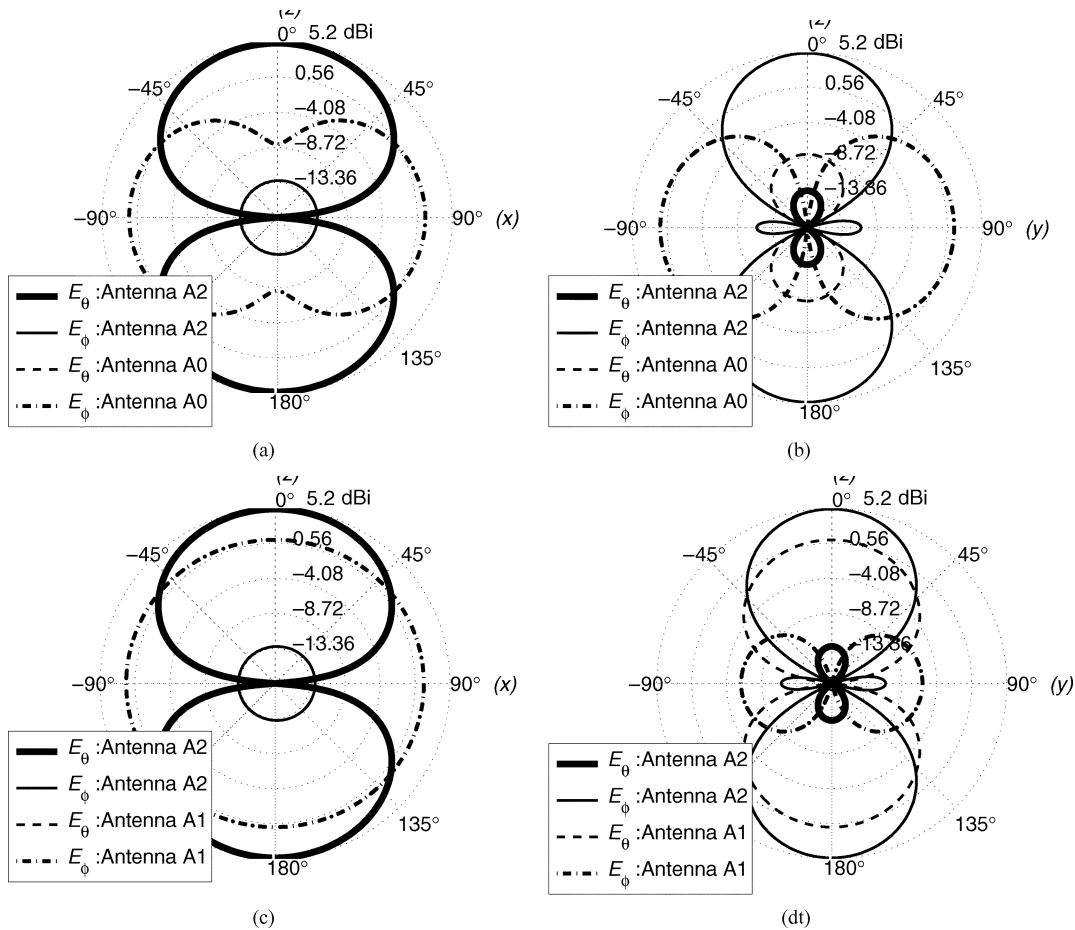


Fig. 6. Radiation pattern comparison between antennas A0, A1 and A2: (a) Antennas A0 and A2 ( $XZ$  plane); (b) antennas A0 and A2 ( $YZ$  plane); (c) antennas A1 and A2 ( $XZ$  plane); (d) antennas A1 and A2 ( $YZ$  plane).

#### IV. INFLUENCE OF THE EYE MODEL ON THE INTRAOCULAR WIRE ANTENNA CHARACTERISTICS

Similar to the case of the patch antenna [6], when the encapsulated intraocular wire antenna is immersed in the eye phantom filled with humor simulant fluid, due to the dielectric loading effect, the wire dipole is de-tuned [16]. The resonant frequency is

lower and the return loss degrades due to an inductive effect in its impedance characteristics.

Thus, for experimental measurements in presence of the model, the intraocular wire antenna was modified to account for the inductive loading effect due to immersion in the eye phantom. The new intraocular antenna was designed so that it exhibits significant capacitive behavior at the desired

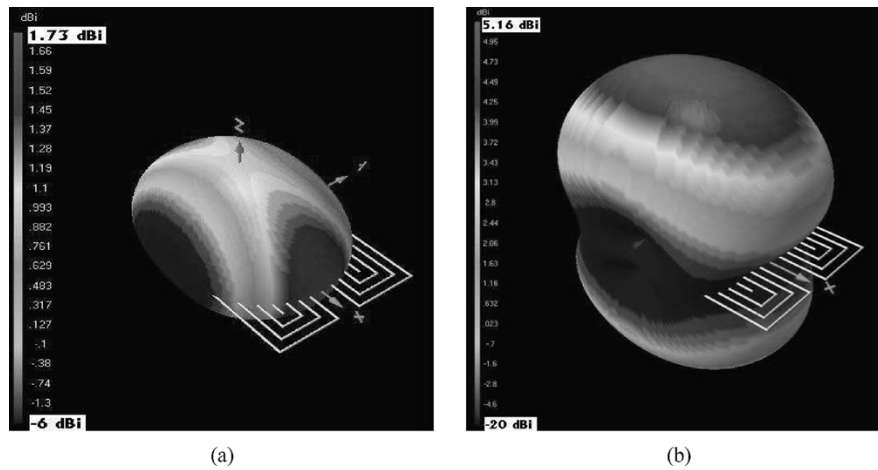


Fig. 7. Total Directivity plots for antennas A1 and A2: (a) Antenna A1 (fundamental mode matched) and (b) antenna A2 (full wave mode matched).

extraocular antenna frequency in free space. This was achieved by altering the lengths of both the arms of the wire dipole until it exhibited capacitive behavior in free space. Thus, when the capacitive wire dipole was packaged and immersed in the eye phantom, the inductive loading influence improved the impedance characteristics and re-tuned its matched resonant frequency to that of the extraocular patch antenna.

Fig. 9 depicts the influence of the eyeball on the antenna characteristics. The implemented re-designed antenna to operate when embedded in the eye model and the one designed to work in free space are shown in Fig. 9(c).

In the NEC simulations of the prototype meander line dipole in free space, a small bandwidth was observed at the matched induced series resonance. On implementation on a thick dielectric substrate ( $\epsilon_r = 9.2$ ,  $h = 1.5$ ) mm, the measured bandwidth improved due to the losses involved. At 1.41 GHz, a 2:1 VSWR bandwidth of approximately 20 MHz was observed as is evident from Fig. 9(b).

## V. COMPARISON BETWEEN PATCH AND WIRE ANTENNAS AS INTRAOCULAR ELEMENTS IN THE DATA TELEMTRY LINK

In our previous work [6], the coupling performance of the data telemetry link employing extraocular and intraocular microstrip patch antennas was investigated at two frequency bands at approximately 1.45 and 2.45 GHz. Therefore, in this work it was of interest to observe the coupling performance of the link with the same external antenna (microstrip patch) but different intraocular antennas. Hence, in the first case the performance of the link was measured with an intraocular microstrip patch element and in the second case with a meander wire dipole as the intraocular element. In this work, this comparison in coupling performance is carried out at approximately 1.4 GHz. In both the cases the intraocular antennas (microstrip patch and meander wire dipole) measured within approximately  $6 \times 6$  mm in occupied area. Since, the link performance results with microstrip patch antenna elements has been outlined in detail in our previous work [6], here we directly compare the coupling measurements obtained with intraocular patch and wire antennas.

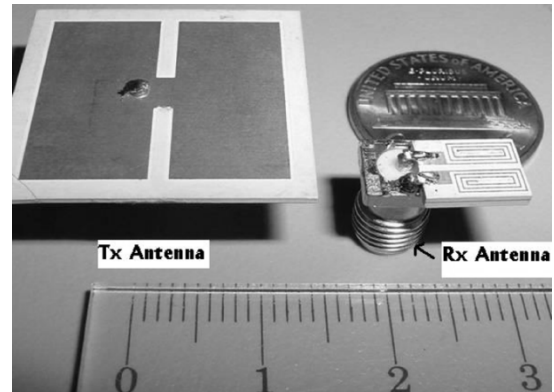


Fig. 8. Implemented  $T_x$  (extraocular) and  $R_x$  (intraocular wire dipole) antennas to operate in the 1.45 GHz frequency band.

### A. Coupling Measurements in Free Space

At a separation of 25 mm in free space (between the extraocular and intraocular antennas), coupling with intraocular patch antenna is experimentally observed to be  $-43.5$  dB while with the intraocular wire dipole antenna, the measured coupling is  $-36.8$  dB. Fig. 10(a) and (b) compare the coupling observed with the patch antenna and the wire dipole antenna.

A significant improvement in coupling (5–6 dB) is observed with the intraocular wire dipole antenna as compared to the patch antenna in free space. This is attributed to the enhancement in broadside directivity of the wire dipole antenna (due to the current phase reversal). The use of an unbalanced feed mechanism may be affecting the coupling result to a minimal extent. Fig. 10(b) depicts the coupling performance as a function of separation which shows improved coupling with the wire dipole antenna.

### B. Coupling Measurements in Presence of the Eye Model

For comparison with an intraocular patch antenna, a similar set of measurements were taken with the re-designed intraocular wire dipole (to account for inductive influence) immersed in the eye model. At a separation of 25 mm (between the extraocular patch antenna and the encapsulated wire dipole immersed in the eye phantom), coupling was observed to be  $-35.8$  dB while

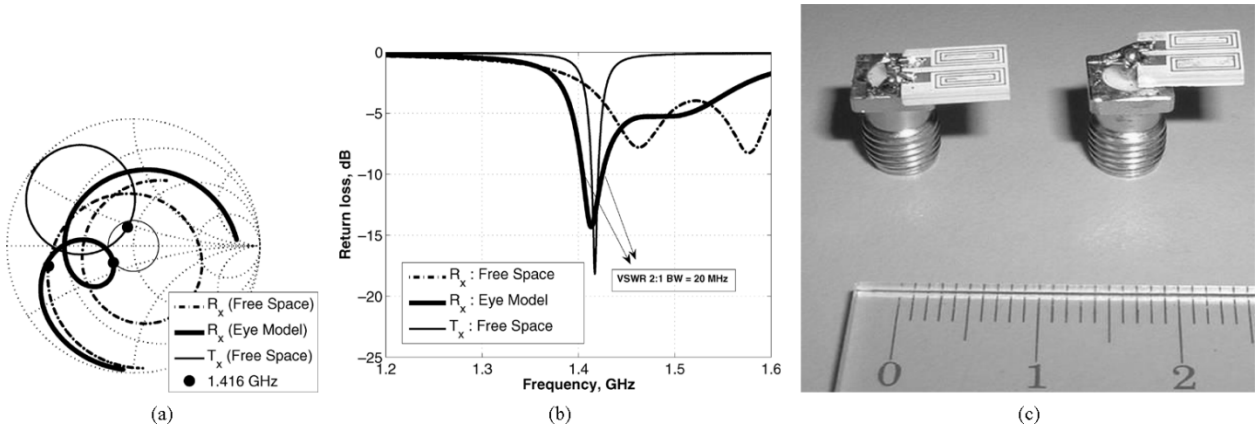


Fig. 9. Measured inductive (dielectric) loading influence of the vitreous humor simulant fluid of the eye model on the  $6 \times 6$  mm intraocular antenna (packaged in a plastic sheath) and immersed to the appropriate depth in the model and the corrected antennas. (a) Measured influence on the  $6 \times 6$  mm meander wire dipole antenna and its correction. (b) Measured return loss characteristics for the wire dipole antenna at 1.41 GHz. (c) The implemented  $R_x$  antennas: On the left is  $R_x$  designed to operate in free space. Shown on the right is the  $R_x$  redesigned to operate when embedded inside the eye model.

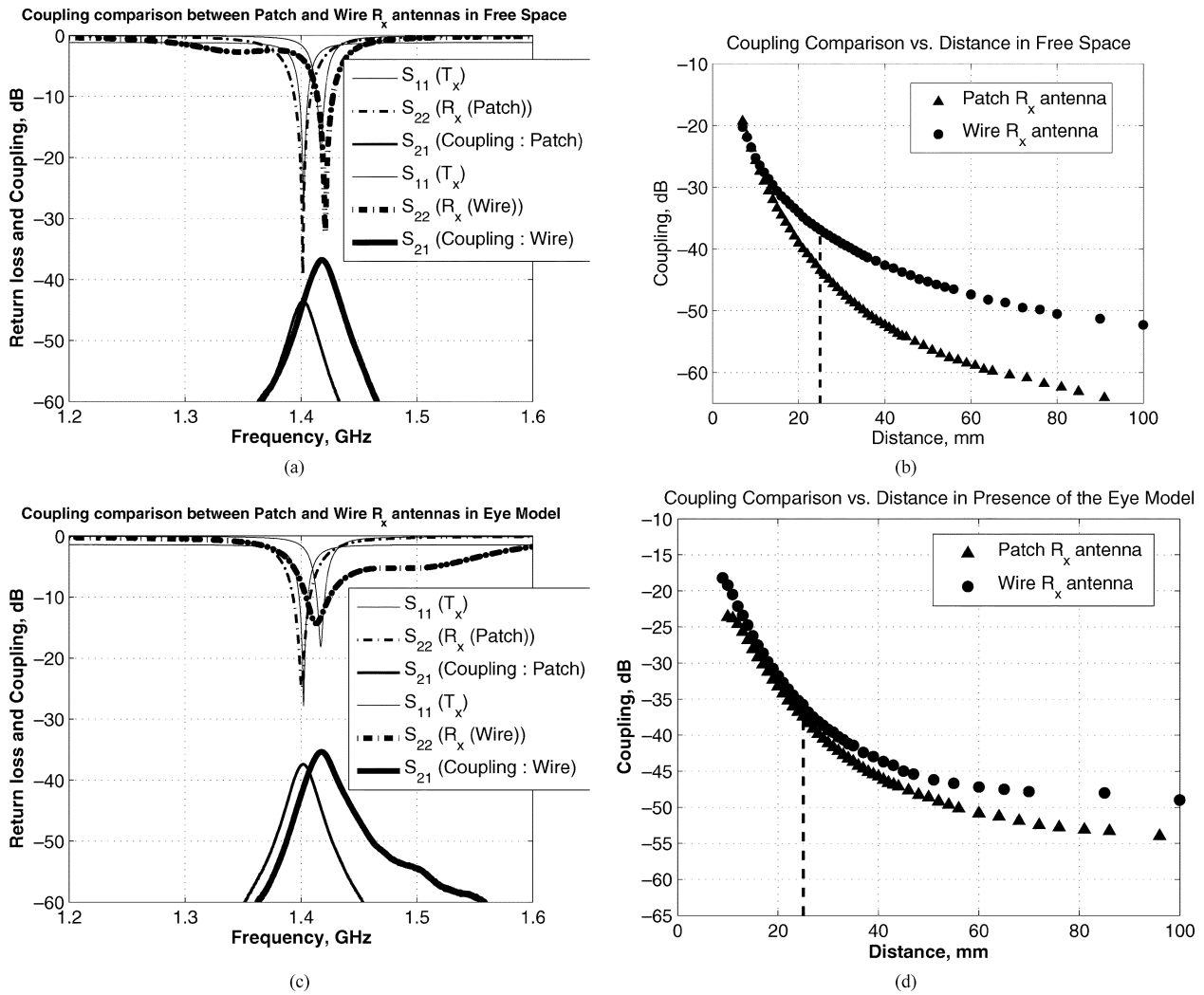


Fig. 10. Comparison of the measured coupling performance between patch and wire dipole antenna as the intraocular element in free space and in presence of the eye model. (a) At a separation of 25 mm in Free Space. (b) As a function of separation in Free Space. (c) At a separation of 25 mm in the presence of the Eye Model. (d) As a function of separation in the presence of the Eye Model.

with the intraocular embedded patch antenna it was observed to be  $-37.8$  dB. Fig. 10(c) and (d) compare the coupling observed with the patch antenna and the wire dipole antenna.

In this case, a minor improvement in coupling with embedded wire antenna is observed (1–3 dB). As is evident from Fig. 10(d), even in presence of the eye model, the performance

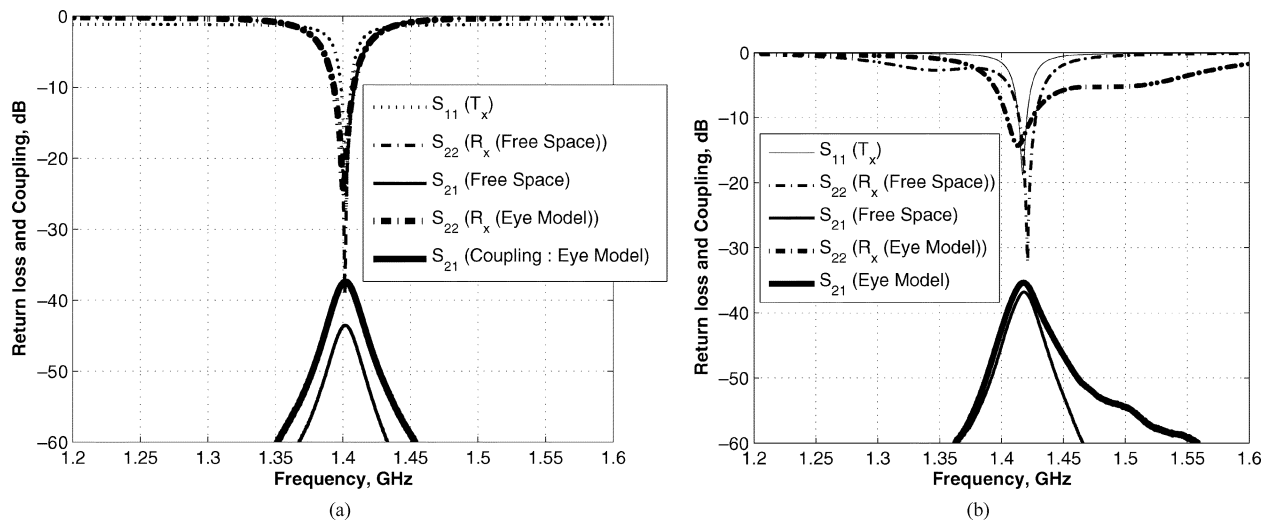


Fig. 11. Comparing the enhancement in coupling due to the dielectric lens effect (with intraocular patch and wire dipole antenna) in the 1.45 GHz band: (a) Improvement with the embedded patch antenna (4–6 dB) and (b) improvement with the embedded wire dipole antenna (1–2 dB).

of the link as a function of separation was better (higher coupling) with the embedded wire dipole than with the embedded patch antenna.

### C. Enhancement in Coupling Performance Due to the Dielectric Lens Effect of the Eye Model

It was reported in [6], that when the intraocular antenna is immersed in the eye model, both numerically and experimentally, an enhancement in coupling was observed. This enhancement was of the order of 4–6 dB in the 1.45 GHz band and 1–2 dB in the 2.45 GHz band for the intraocular patch antennas. This effect was attributed to the fact that the curvature of the eyeball and the head tissues may act as a dielectric lens and enhance coupling performance.

Hence, it was of interest to observe the enhancement in coupling with the wire dipole and compare the results with the corresponding patch antenna results. Fig. 11 compares the improvement observed with intraocular wire dipole and patch antenna. As depicted in Fig. 11(a), with the patch antenna element, the improvement was of the order of 4–6 dB while as seen from Fig. 11(b) the improvement was lesser of the order of 1–2 dB with the intraocular wire dipole antenna. This is attributed to the fact that the high directivity and polarization characteristics of the wire dipole antenna may be more adversely affected than for the patch antenna (on immersion in the eye model). A comprehensive study on the discrepancy of the radiation characteristics of compact patch and wire antennas embedded in such highly lossy dielectric matter is still underway.

## VI. CONCLUSION

We have presented a method of matching a highly compact planar meander line dipole antenna at its higher order mode (full wave resonance). It was demonstrated that for specific extremely compact meander wire antenna geometries, a minor

offset in the feed point introduced by shortening one of the dipole arms can induce a current phase reversal and provide an impedance match while retaining the feed point at the structure's symmetrical center. Phase reversal on wire antenna configurations possessing a high degree of current vector alignment among adjacent wire lengths can improve the broadside directivity, albeit at a deterioration in the bandwidth.

An edge fed planar meander line dipole antenna measuring  $5.25 \times 5.25 \times 1.5$  mm is implemented to operate at 1.41 GHz for its use as an intraocular element in a retinal prosthesis. This wire dipole antenna is impedance matched using the current phase reversal technique. Coupling measurements are performed both in free space and with the wire dipole antenna embedded in an eye model and compared with corresponding results with an embedded patch antenna. At a fixed separation of 25 mm, the coupling measurements in free space and in the presence of the eye model are  $-36.8$  dB and  $-35.8$  dB respectively with the receiving wire antenna.

It is shown here that compact wire dipole antennas with appropriate dimensions and coupling performance can be designed, implemented and matched to any system impedance for their use as implanted antennas in a retinal prosthesis or other similar biomedical telemetry applications.

## REFERENCES

- [1] E. Margalit, M. Maia, J. D. Weiland, R. J. Greenberg, G. Y. Fujii, G. Torres, D. V. Piyathaisere, T. M. O'Hearn, W. Liu, G. Lazzi, G. Dagnellie, D. A. Scribner, E. de Juan Jr., and M. S. Humayun, "Retinal prosthesis for the blind," *Survey of Ophthalmology*, vol. 47, no. 4, pp. 335–356, 2002.
- [2] E. Zrenner, "Will retinal implants restore vision?," *Science Mag.*, vol. 295, pp. 1022–1025, Feb. 2002.
- [3] W. Liu, M. S. Humayun, E. McGucken, E. de Juan Jr., J. D. Weiland, S. C. DeMarco, and M. Clements, "Multiple unit artificial retina chipset system to benefit the visual impaired," in *Intelligent Systems for the Disabled*, N. Theodorescu, Ed. Boca Raton, FL: CRC Press, 2000, ch. 2.
- [4] M. V. Narayanan, J. F. Rizzo, D. Edell, and J. L. Wyatt, "Development of a silicon retinal implant: Cortical evoked potentials following focal stimulation of the rabbit retina with light and electricity," *Investigative Ophthalmology and Visual Science*, vol. 35, p. 1380, 1994.

- [5] W. Liu, K. Vichienchom, M. Clements, S. C. DeMarco, C. Hughes, E. McGucken, M. S. Humayun, E. de Juan Jr., J. D. Weiland, and R. J. Greenberg, "A neuro-stimulus chip with telemetry unit for retinal prosthetic device," *IEEE J. Solid-State Circuits*, vol. 35, no. 10, pp. 1487–1497, Oct. 2000.
- [6] K. Gosalia, G. Lazzi, and M. Humayun, "Investigation of a microwave data telemetry link for a retinal prosthesis," *IEEE Trans. Microw. Theory Tech.*, vol. 52, no. 7, pp. 1925–1933, Aug. 2004.
- [7] S. R. Best and J. D. Morrow, "On the significance of current vector alignment in establishing the resonant frequency of small space-filling wire antennas," *IEEE Antennas Wireless Propag. Lett.*, vol. 2, pp. 201–204, 2003.
- [8] —, "The effectiveness of space-filling fractal geometries in lowering resonant frequency," *IEEE Antennas Wireless Propag. Lett.*, vol. 1, pp. 112–115, 2002.
- [9] L. J. Chu, "Physical limitations on omni-directional antennas," *J. Appl. Phys.*, vol. 19, pp. 1163–1175, Dec. 1948.
- [10] R. F. Harrington, "Effect of antenna size on gain, bandwidth, and efficiency," *J. Res. NBS*, vol. 64D, pp. 1–12, Jan. 1960.
- [11] H. A. Wheeler, "Fundamental limitations of small antennas," *Proc. IRE*, vol. 35, pp. 1479–1488, 1947.
- [12] C. Puente, J. Romeu, and A. Cardama, "The koch monopole: A small fractal antenna," *IEEE Trans. Antennas Propag.*, vol. 48, no. 11, pp. 1773–1781, Nov. 2000.
- [13] NEC Win Pro. Nittany-Scientific. [Online]. Available: [www.nittany-scientific.com/nwp/](http://www.nittany-scientific.com/nwp/)
- [14] J. Zhu, A. Hoorfar, and N. Engheta, "Bandwidth, cross-polarization and feed-point characteristics of matched Hilbert antennas," *IEEE Antennas Wireless Propag. Lett.*, vol. 2, pp. 2–5, 2003.
- [15] W. L. Stutzman and G. A. Thiele, *Antenna Theory and Design*, 2nd ed. New York: Wiley, 1998.
- [16] I. J. Bahl and P. B. S. Stuchly, "Design of microstrip antennas covered with a dielectric layer," *IEEE Trans. Antennas Propag.*, vol. 30, no. 2, pp. 314–318, Mar. 1982.



**Keyoor Gosalia** (S'01–M'05) received the B.E. degree in electronics from Sardar Patel University, Gujarat, India, and the M.S. and Ph.D. degrees in electrical engineering from North Carolina State University, Raleigh, in 2001 and 2004, respectively.

From January 2001 to August 2004, he was a Graduate Research Assistant in the Electrical Engineering department at North Carolina State University. Since October 2004, he has been with General Dynamics C4 Systems (Satcom Technologies), Kilgore, TX, as an RF Engineer. His research

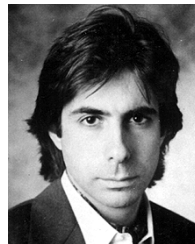
interests include numerical electromagnetics, bioelectromagnetics, novel design techniques for small antennas and human body implantable antennas, planar ultrawide-band antenna systems for improving multiple-input-multiple-output (MIMO) channel capacity, earth station antenna systems, microwave feed systems, and waveguide components.



**Mark S. Humayun** (M'97) received the M.D. degree from Duke University Medical School, Durham, NC, in 1989 and the Ph.D. degree in biomedical engineering from the University of North Carolina, Chapel Hill, in 2001.

He served a residency in ophthalmology at the Duke Eye Center and fellowships with the Retinovascular Center, Johns Hopkins Hospital, and in vitreoretinal surgery with the Johns Hopkins Medical Institution. From 1995 to 2001, he was an Assistant Professor of ophthalmology with the Johns Hopkins

Wilmer Eye Institute. He is currently Professor of Ophthalmology with the Keck School of Medicine, University of Southern California, Los Angeles, and Associate Director of Research with the Doheny Retina Institute, Los Angeles, CA, where he provides patient care while developing innovative techniques and diagnostics to treat blinding retinal disorders. His quest to find a cure for currently untreatable blinding retinal diseases led him to become one of the primary creators of the intraocular retinal prosthesis that was recently implanted into the first patient in a Food and Drug Administration (FDA) investigational device study. In August 2001, he joined the Doheny Retina Institute, Doheny Eye Institute, where he holds three appointments: ophthalmology, biomedical engineering and cell and neurobiology. His research has focused on microelectronic solutions for severe retinal disease.



**Gianluca Lazzi** (S'94–M'95–SM'99) received the Dr.Eng. degree in electronics from the University of Rome "La Sapienza," Rome, Italy, in 1994, and the Ph.D. degree in electrical engineering from the University of Utah, Salt Lake City, in 1998.

He is currently an Associate Professor with the Department of Electrical and Computer Engineering, North Carolina State University (NCSU), Raleigh, where, from 1999 to 2003, he was an Assistant Professor. He has been a Visiting Researcher with the Italian National Board for New Technologies,

Energy, and Environment (ENEA) (1994), a Visiting Researcher with the University of Rome "La Sapienza" (1994–1995), and a Research Associate (1995–1998) and Research Assistant Professor (1998–1999) with the University of Utah. He has authored or coauthored over 100 international journal papers or conference presentations on implantable devices, medical applications of electromagnetic fields, antenna design, FDTD modeling, dosimetry, and bioelectromagnetics.

Dr. Lazzi is the Vice Chair of Commission K (Electromagnetics in Biology and Medicine) of the U.S. National Committee of the International Union of Radio Science (URSI). He was the recipient of the 1996 Curtis Carl Johnson Memorial Award for the best student paper presented at the 18th Annual Technical Meeting of the Bioelectromagnetics Society (BEMS), a 1996 International Union of Radio Science (URSI) Young Scientist Award, the 1996 Curtis Carl Johnson Memorial Award for the Best Student Paper presented at the 18th Annual Technical Meeting of the Bioelectromagnetics Society, a 2001 Whitaker Foundation Biomedical Engineering Grant for Young Investigators, a 2001 National Science Foundation (NSF) CAREER Award, a 2003 NCSU Outstanding Teacher Award, the 2003 NCSU Alumni Outstanding Teacher Award, and the 2003 ALCOA Foundation Engineering Research Achievement Award. He is an Associate Editor for the *IEEE ANTENNAS AND WIRELESS PROPAGATION LETTERS* and served as a Guest Editor for the "Special Issue on Biological Effects and Medical Applications of RF/Microwaves" of the *IEEE TRANSACTIONS ON MICROWAVE THEORY AND TECHNIQUES* in 2004. He is listed in *Who's Who in the World*, *Who's Who in America*, *Who's Who in Science and Engineering*, *Dictionary of International Biographies*, and *2000 Outstanding Scientists of the 20th Century*.